Synthesis and Characterization of Core Cross-Linked Star Clusters by Conventional Free-Radical Polymerization

Tor Kit Goh,† Adrian P. Sulistio,† Anton Blencowe,† Jeffery W. Johnson,‡ and Greg G. Qiao*,†

Polymer Science Group, Department of Chemical and Biomolecular Engineering, University of Melbourne, Parkville, Victoria 3010, Australia, and DuPont Automotive Systems, 400 N. Grosebeck Highway, Mt. Clemens, Michigan 48043

Received May 1, 2007; Revised Manuscript Received August 21, 2007

ABSTRACT: Core cross-linked star (CCS) clusters consisting of linear poly(methyl methacrylate) (PMMA) segments surrounding multiple, dispersed poly(divinylbenzene) (PDVB) cores have been synthesized by conventional free-radical polymerization via a "core-first" method. This unique macromolecular structure is akin to a cluster of several CCS polymers (a star polymer with a single, densely cross-linked core) that are covalently bonded together by linear core-to-core PMMA segments and retain excellent solubility even at very high molecular weights. This study provides evidence to the proposed "core-first" mechanism and subsequent CCS cluster formation by comparison to linear PMMA and model CCS polymers synthesized by atom transfer radical polymerization (ATRP). Characterization by UV−vis spectrophotometry, proton nuclear magnetic resonance (^{1}H NMR), dynamic light scattering (DLS), and thermal analysis verified the formation of PMMA−PDVB CCS clusters and elucidated their macromolecular structure. Molecular weights of between 5000 and 20 000 kDa were achievable by selection of the appropriate formulation. Light scattering studies showed that CCS clusters have a hydrodynamic radius of between 20 and 50 nm, and this size is tunable on the basis of solvent choice.

Introduction

Polymers with well-defined macromolecular architectures have been the subject of intense academic and industrial research as a result of their distinctive properties compared to their linear counterparts. For example, branched[1] and star macromolecules[2−7] have been shown to exhibit distinctive rheology, solubility, miscibility, and reactivity characteristics. One such type of macromolecule is the core cross-linked star (CCS) polymer,[8] which possesses linear arms that radiate from a densely cross-linked core. Such defined polymers have been synthesized by nitroxide-mediated polymerization (NMP),[2] atom transfer radical polymerization (ATRP),[3−5] reversible addition−fragmentation chain transfer (RAFT),[6] and anionic polymerization[7] methodologies. The common denominator is the synthetic approach, which involves the formation of "living" linear polymers by exclusive chain growth of monovinyl monomer(s) followed by reaction with a multifunctional monomer. This method to form precise monodisperse macromolecules is called the "arms-first" method. The controlled architecture endows specific properties that make them suitable for applications in high-performance motor oils,[7] drug delivery,[9] paint formulations,[10] and nanostructured surfaces.[11] More recently, the "arms-first" synthetic approach has been used in conjunction with ring-opening polymerization (ROP) to form selectively degradable CCS polymers.[12,13]

While the synthesis of CCS polymers via living radical polymerization offers a high degree of control over structure, branching, and compositional distribution, there remains major obstacles for process scale-up. In the case of ATRP, stringent purity requirements for reagents and subsequent removal of metal complexes from the product are but two examples. Thus, the introduction of conventional free-radical polymerization (FRP) methods for the formation of similar macromolecules[10,14,15] (such as microgels) may allow for commercialization without the complications that limit scale-up of living radical methods. The main synthetic methods adopted using FRP to form microgels thus far are emulsion copolymerization[14] and solution copolymerization[15,16] of mono- and polyfunctional monomers.

In this study, the "core-first" FRP approach was investigated. Core particles comprising of loosely cross-linked polymer with unreacted double bonds were synthesized by homopolymerization of divinylbenzene (DVB) and were then polymerized with methyl methacrylate (MMA) to form a new class of polymer, i.e., CCS clusters, so-called because they consist of a number of stars covalently bonded by linear polymers. The unique architecture is akin to a cluster of CCS polymers that may be synthesized up to several million daltons without phase separation from the solvent, which is indicative of the high solubility characteristics imparted by the linear segments of the cluster. Like products of emulsion polymerization of mono- and divinyl monomers, CCS clusters have multiple high-density regions within a less-dense network; however, CCS clusters will dissolve in common organic solvents whereas the emulsion particles require dispersion and stabilization with surfactants. CCS polymers of $(PMMA/x)_f$−PDVB and $(PMMA/x)_f$−PEGDMA (where PDVB and poly(ethylene glycol dimethacrylate) (PEGDMA) represent the core constituents, $(PMMA/x)$-$_f$ represents the arm constituent, arm M_w in kDa (x), and average number of arms (f)) were synthesized by ATRP and used as model compounds. The full characterization of these polymers is presented herein.

The synthesis and characterization of CCS clusters is an important step in understanding the influence of polymer architecture on bulk and solution behavior. In particular, the tunable density of the CCS cluster according to solvent selection may lead to novel nanoparticles with low viscosities.

* Corresponding author: e-mail gregghq@unimelb.edu.au.
† University of Melbourne.
‡ DuPont Automotive Systems.

10.1021/ma070996z CCC: $37.00
Published on Web 10/09/2007

Experimental Section

Materials. The monomers divinylbenzene (DVB, technical grade, 80%) and methyl methacrylate (MMA, 99%+) were purchased from Aldrich and purified by passing through a column of basic alumina or inhibitor remover (Aldrich), respectively. 2,2-Azobis(2-methylpropionitrile) (AIBN) (DuPont Australia Vazo 64) was recrystallized from diethyl ether and stored below 4 °C. *p*-Toluenesulfonyl chloride (TsCl, 99%+) (Aldrich) was dissolved in chloroform, diluted with petroleum ether (bp 40−60 °C), treated with charcoal, filtered, concentrated, and collected by filtration. Copper(I) bromide, hydroquinone (HQ, 99%), 2,2′-bipyridine (bpy, 99%+), and *N*,*N*,*N*′,*N*′,*N*″-pentamethyldiethylenetriamine (PMDETA, 99%) were purchased from Aldrich and used without further purification. Toluene, *p*-xylene, methanol, and tetrahydrofuran (THF) were obtained from British Drug House (BDH) Chemical Ltd. and used without further purification.

Characterization. ^{1}H NMR spectroscopic analysis was performed on a Varian Unity 400 (400 MHz) spectrometer (using tetramethylsilane (TMS) and the deuterated solvent as lock and residual solvent) while ^{13}C NMR spectroscopic analysis was performed on a Varian Unity 400 (100 MHz) spectrometer (using the deuterated solvent as lock and residual solvent). Polymer concentrations were fixed at 50 mg/mL of deuterated solvent containing 1% v/v of TMS. UV−vis analysis was performed on a Shimadzu UV−vis scanning spectrophotometer (UV-2101 PC) with a CPS-260 6-cell positioner and temperature controller (set at 20 °C) using THF as the solvent. Gel permeation chromatography (GPC) analysis was performed on a system fitted with a Wyatt DAWN DSP multiangle laser light scattering (MALLS) detector (λ = 690 nm, 30 mW), a Wyatt OPTILAB EOS interferometric refractometer (λ = 690 nm), and a Shimadzu SPD-10A UV−vis detector using three Phenomenex phenogel columns (porosities of 500, 10^4, and 10^6 Å) and GPC-grade THF (conducted at 30 °C and a flow rate of 1 mL min^{-1}). GPC-MALLS was calibrated by d*n*/d*c* of pure solvent (λ = 690 nm). Molecular weights were calculated using Astra software (Wyatt Technology Corp.) based on injected mass values and the assumption of 100% mass recovery. Gas chromatography−mass spectroscopy (GCMS) was performed on a Shimadzu GC-17A gas chromatograph with a Shimadzu GCMS-QP5000 electron ionization mass spectrometer and Zebron ZB-5 capillary column (solid phase 5% phenyl−95% dimethylpolysiloxane, 30 m × 0.25 mm × 0.25 μm). The injection and interface temperatures were 250 and 230 °C, respectively, and the temperature program was as follows: 40−55 °C at 7 °C/min, 55−235 °C at 10 °C/min. Dynamic light scattering (DLS) measurements were performed on a Malvern high performance particle sizer (HPPS) with a He−Ne laser (633 nm) at an angle of 173°. All DLS measurements were performed at 25 °C. Differential scanning calorimetry (DSC) was performed on a TA Instruments model 2920 modulated DSC with a heating rate of 10 °C min^{-1} under nitrogen flow. DSC calibration was performed using indium. Determination of T_g was achieved by using the Universal Analysis program (TA Instruments) to determine the onset, inflection, and end points on the heat flow curve. Thermogravimetric analysis (TGA) was performed on a Perkin-Elmer thermogravimetry/differential thermal analyzer with a heating rate of 10 °C min^{-1} under nitrogen flow. All samples were dried under vacuum (0.05 mmHg) before DSC and TGA analysis.

Synthesis of PDVB Cores. AIBN (26.3 mg, 0.16 mmol), DVB (1.11 mL, 7.68 mmol), and toluene (20 mL) were added to a dry Schlenk tube with a magnetic stirrer bar and sealed. The mixture was then subjected to three freeze−pump−thaw cycles and back-filled with argon. The tube was heated at 65 °C for 1 h, and then hydroquinone (35.2 mg, 0.32 mmol) dissolved in THF (10 mL) was added to quench the reaction. The reaction solution was diluted with a 10-fold excess of THF and precipitated into cold methanol (−18 °C). The precipitate was removed from the mother liquor by filtration, washed twice with methanol, and dried in a vacuum desiccator (<0.05 mmHg) for 5 h to afford the desired PDVB cores as a white solid, 48.0 mg (5%). ^{1}H NMR (400 MHz, $CDCl_3$, TMS): δ_H 7.06 (*s*, Ar**H**), 6.75−6.66 (br m, Ar**C**H$_2$), 5.78−5.73 (br m, CH**C**HH), 5.27−5.12 (br m, CHCH**H**), 2.30 (s, C**H**), 1.51 ppm (s, C**H**$_2$). ^{13}C NMR (100 MHz, $CDCl_3$, TMS): δ_C 149.0−142.2 (br m, Ar**C**C), 138.1−136.2 (br m, Ar**C**C + ArC**C**H), 131.5−124.9 (br m, Ar**C**H), 114.1−113.2 (br m, CH**C**H$_2$), 48.3−39.1 ppm (br m, **C**H$_2$ + **C**H). GPC-MALLS: M_w = 81.0 kDa, PDI = 1.6.

Synthesis of PMMA−PDVB CCS Cluster. AIBN (15.9 mg, 0.10 mmol), MMA (1.03 mL, 9.67 mmol), PDVB cores (30.0 mg, 0.37 μmol), and toluene (6.7 mL) were added to a dry Schlenk tube with a magnetic stirrer bar and sealed. The mixture was then subjected to three freeze−pump−thaw cycles and back-filled with argon. The tube was heated at 65 °C for 50 h, and then hydroquinone (21.1 mg, 0.19 mmol) dissolved in THF (10 mL) was added to terminate the reaction. The reaction solution was diluted with a 10-fold excess of THF and precipitated into cold methanol (−18 °C). The precipitate was removed from the mother liquor by filtration, washed twice with methanol, and dried in a vacuum desiccator (<0.05 mmHg) for 5 h to afford a mixture of CCS cluster and linear PMMA as a white solid, 0.92 g (95%). GPC-MALLS: Peak 1 (88%): M_w = 84 kDa, PDI = 2.4. Peak 2 (12%): M_w = 3800 kDa, PDI = 2.2.

Pure CCS clusters were obtained by fractional precipitation, which was carried out by removing excess solvent from the reaction solution in vacuo followed by incremental addition of cold methanol (−18 °C). The precipitate formed was removed from the mother liquor by filtration, washed twice with methanol, and dried in a vacuum desiccator (<0.05 mmHg) for 5 h. The process was repeated with the filtrate until several fractions are obtained. ^{1}H NMR (400 MHz, $CDCl_3$, TMS): δ_H 3.57 (br s, OC**H**$_3$), 2.04−1.72 (br m, C**H**$_2$), 1.43−1.35 (br m, C**H**$_3$), 1.24−1.19 (br m, C**H**$_3$), 0.97 (br s, C**H**$_3$), 0.82 ppm (br s, C**H**$_3$). ^{13}C NMR (100 MHz, $CDCl_3$, TMS): δ_C 178.1 (**C**O), 177.8 (**C**O), 177.1 (**C**O), 176.9 (**C**O), 54.4 (**C**H$_2$), 54.2 (**C**H$_2$), 52.9 (O**C**H$_3$), 52.7 (O**C**H$_3$) , 52.5 (O**C**H$_3$) , 51.8 (O**C**H$_3$), 44.8 (**C**CH$_3$), 44.5 (**C**CH$_3$), 18.7 (**C**H$_3$), 16.4 ppm (**C**H$_3$). GPC-MALLS: M_w = 6753 kDa, PDI = 1.24.

Kinetic Study of CCS Cluster Formation. MMA (29.6 g, 0.28 mol) and PDVB cores (1.00 g, 1.23 μmol) were dissolved in toluene (172 mL) and placed in a three-neck round-bottom flask fitted with a water-cooled condenser and an addition funnel. Argon was then bubbled through the solution with stirring for 1 h. Separately, AIBN (0.45 g, 2.78 mmol) was dissolved in toluene (20 mL) and added to the addition funnel, and argon was bubbled through the solution for 1 h. The reaction mixture was then heated to 65 °C, and the content of the addition funnel was added to the round-bottom flask. Periodically, 0.5 mL samples of the reaction mixture was taken using a gastight syringe and immediately added to a mixture of THF (5 mL) and HQ (31.0 mg, 0.28 mmol). After 50 h, the argon flow was turned off, and hydroquinone (0.61 g, 5.56 mmol) dissolved in THF (100 mL) was added to terminate the reaction. The reaction solution was diluted with a 10-fold excess of THF and precipitated into cold methanol (−18 °C). The precipitate was removed from the mother liquor by filtration, washed twice with methanol, and dried in a vacuum desiccator (<0.05 mmHg) for 5 h to afford a mixture of the CCS clusters and linear PMMA as a white solid, 27.5 g (95%). GPC-MALLS: Peak 1 (76%): M_w = 49.0 kDa, PDI = 4.28. Peak 2 (24%): M_w = 5254 kDa, PDI = 1.78.

Synthesis of Living Poly(methyl methacrylate) (PMMA). TsCl (550 mg, 2.88 mmol), copper(I) chloride (172 mg, 1.12 mmol), PMDETA (0.22 mL, 1.12 mmol), MMA (12.0 g, 0.12 mol), and *p*-xylene (17.2 mL) were added to a dry Schlenk tube with a magnetic stirrer bar and sealed. The mixture was then subjected to three freeze−pump−thaw cycles and back-filled with argon. The tube was heated at 80 °C for 90 h. The reaction was quenched with a 10-fold excess of THF and passed through a plug of basic alumina to remove the catalyst followed by precipitation in cold methanol (−18 °C). The precipitate was removed from the mother liquor by vacuum filtration, washed twice with methanol, and dried in a vacuum desiccator (<0.05 mmHg) for 5 h. This afforded the living PMMA as a white solid, 2.59 g (21.5%). ^{1}H NMR (400 MHz, $CDCl_3$): δ_H 7.85−7.67 (m, Ar**H**), 7.40−7.29 (m, Ar**H**), 3.71 (br

Scheme 1. Synthesis of Poly(divinylbenzene) (PDVB) Cores by Conventional Free-Radical Polymerization Using 2,2-Azobis(2-methylpropionitrile) (AIBN) as the Initiator

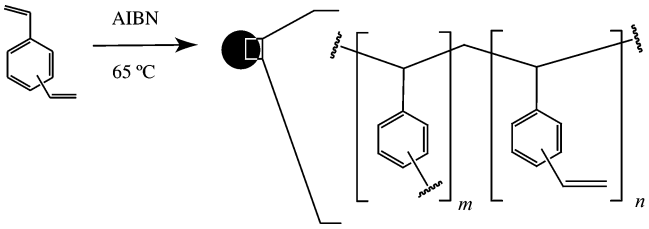

s, OC**H**$_3$), 3.67 (br s, SO_2C**H**$_2$), 3.60 (br s, OC**H**$_3$), 3.48 (br s, OC**H**$_3$), 2.45 (br s, ArC**H**$_3$), 2.09−1.81 (m, C**H**$_2$), 1.43 (br s, C**H**$_3$), 1.21 (br s, C**H**$_3$), 1.01 (br s, C**H**$_3$), 0.83 ppm (br s, C**H**$_3$). ^{13}C NMR (100 MHz, $CDCl_3$): δ_C 178.3 (**C**O), 178.0 (**C**O), 177.7 (**C**O), 177.0 (**C**O), 176.8 (**C**O), 176.0 (**C**O), 129.7 (Ar**C**C), 127.6 (Ar**C**H), 127.5 (Ar**C**H), 54.3 (O**C**H$_3$), 54.2 (O**C**H$_3$), 54.1(O**C**H$_3$), 51.7 (**C**H$_2$), 44.7 (**C**(CH$_3$)$_2$), 44.4 (**C**(CH$_3$)$_2$), 21.5 (**C**H$_3$), 20.9 (**C**H$_3$), 18.8 (**C**H$_3$), 18.6 (**C**H$_3$), 16.3 ppm (**C**H$_3$). GPC-MALLS: M_w = 9.8 kDa, PDI = 1.11.

Synthesis of CCS Polymers. ATRP and the "arms-first" method were employed to synthesize these polymers using previously established conditions.[3] The resulting mixtures were purified by fractional precipitation, and the isolated CCS polymers were dried under high vacuum (0.05 mmHg) for 5 h. $(PMMA/21\ kDa)_{21}$−PEGDMA; GPC−MALLS, M_w = 530 kDa, PDI = 1.06, $M_{w,PEGDMA\ core}$ = 89 kDa. $(PMMA/10\ kDa)_{108}$−PDVB; GPC−MALLS, M_w = 1345 kDa, PDI = 1.56, $M_{w,PDVB\ core}$ = 291 kDa. Calculation methods for f and $M_{w,core}$ have been previously published.[13]

Results and Discussion

Formation of CCS clusters by FRP is a two-step synthetic process involving (i) the synthesis of a soluble "core" (globular polymeric particles with pendant unreacted vinylic moieties) followed by (ii) reaction with monovinyl monomers to form the CCS cluster.

Synthesis of PDVB Cores. The synthesis of polymeric particles with unreacted pendant double bonds by FRP was achieved by homopolymerization of divinylbenzene (DVB) (Scheme 1) in very dilute solutions (<5% w/v). The solvent cage effect was prevalent at these low concentrations to the extent that macrogelation was avoided and soluble, loosely cross-linked PDVB cores could be isolated by termination of the polymerization with hydroquinone. The amount of unreacted pendant double bonds present in the PDVB cores was dependent on the initial concentration of DVB monomer, as concluded by Okay et al.[16]

Table 1 shows the results of FRP of DVB. It was found that the higher the concentration of DVB monomer, the higher the amount of unreacted pendant double bonds in the resulting core. PDVB cores synthesized from 1% w/v DVB in toluene were unreactive toward further polymerization, whereas further polymerization was possible with PDVB cores prepared via 5% w/v DVB formulations. The extent of reaction was controlled by termination of the polymerization with hydroquinone to prevent formation of insoluble particles. The optimum conditions for PDVB core formation were achieved at a DVB concentration of 5% w/v and a reaction time of 1 h at 65 °C. GPC-MALLS was used to accurately determine the absolute molecular weight of the PDVB cores because a mass-sensitive detector (e.g., refractive index (RI) detector) used alone may underestimate the molecular weight values.[13] Thus, the PDVB cores **2A** had a M_w of 85.6 kDa and a PDI of 1.6. In addition, proton nuclear magnetic resonance (^{1}H NMR) spectroscopic analysis of the PDVB cores (purified by precipitation) indicated the presence of unreacted pendant double bonds.

Table 1. Experimental Data for Synthesis of Poly(divinylbenzene) (PDVB) Cores by Conventional Free-Radical Polymerization (FRP)

polymer[a]	DVB[b] (% w/v)	n_{DVB}/n_{AIBN}	t_{rxn}[c] (h)	M_w[d] (kDa)	PDI[d]
1A	1	10	10.0	85.6	1.04
1B	1	10	12.5	165.0	1.43
1C	1	10	15.0	354.0	2.57
1D	1	10	20.0	1400.0	4.21
2A	5	50	1.0	81.0	1.60
2B	5	50	2.5	gel[e]	
2C	5	50	5.0	gel[e]	

[a] FRP of divinylbenzene (DVB) was carried out in toluene and initiated by 2,2-azobis(2-methylpropionitrile) (AIBN) at 65 °C. [b] The concentration of DVB is expressed as % w/v = (mass of DVB/volume of solvent) × 100%. [c] Polymerization was terminated by addition of hydroquinone dissolved in THF. [d] Weight-average molecular weight (M_w) and polydispersity index (PDI) were determined by gel permeation chromatography−multiangle laser light scattering (GPC−MALLS). [e] Highly cross-linked particles of PDVB were formed which were insoluble in common organic solvents.

Scheme 2. Synthesis of CCS Clusters from Poly(divinylbenzene) (PDVB) Cores and Methyl Methacrylate (MMA) by Conventional Free-Radical Polymerization Using 2,2-Azobis(2-methylpropionitrile) (AIBN) as the Initiator

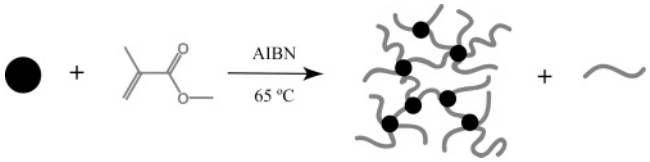

Synthesis of CCS Clusters. PDVB cores **2A** with unreacted pendant double bonds were reacted further with monovinyl monomers to form a mixture of CCS clusters and linear polymer (Scheme 2). Typical GPC chromatograms of the unreacted PDVB cores and CCS clusters are presented in parts a and b of Figure 1, respectively. PDVB cores possess a UV maxima (λ = 291 nm),[17] which results from the aromatic moieties and coincides with the differential refractive index (DRI) and light scattering (LS) peaks from GPC-MALLS analysis. After cluster formation, the position of the UV absorption is shifted to a lower elution time, coinciding with the high-M_w DRI and LS peaks. Thus, the key indicator of the presence of CCS clusters is the UV trace. In comparison, linear PMMA does not absorb at this wavelength, and therefore any UV absorbance detected is solely due to the PDVB cores. The complete shift of the PDVB core UV absorption indicates that the PDVB cores were reactive to further polymerization and were fully incorporated into the clusters (as there was no UV absorption at the initial elution times).

Isolation of CCS clusters was achieved by fractional precipitation. GPC with an online UV−vis detector was used to observe the migration of the UV absorption of the pure CCS cluster compared to the PDVB core precursor (Figure 2a). The shift in position of the UV absorption indicates the full incorporation of PDVB cores into the cluster. Dynamic light scattering (DLS) and ^{1}H NMR spectroscopic analyses were also used to characterize the fractionated CCS clusters. DLS of PDVB cores and fractionated CCS clusters are presented in Figure 2b, where the mean diameters were determined to be 7.2 and 51.3 nm, respectively. ^{1}H NMR spectroscopic analysis of the PDVB cores and fractionated CCS clusters are presented in Figure 3. The ^{1}H NMR spectrum of PDVB cores (Figure 3a) indicated the presence of unreacted pendant double bonds as revealed by three broad resonances at approximately δ_H 5.2, 5.7, and 6.7 ppm corresponding to the vinylic group protons. The ^{1}H NMR spectrum of the fractionated CCS cluster (Figure 3b) is

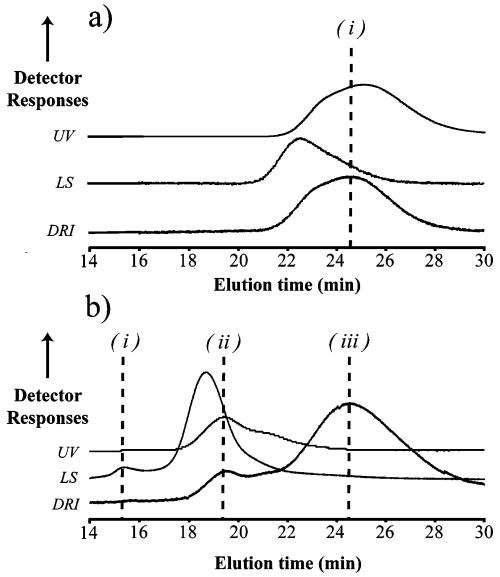

Figure 1. GPC chromatograms for (a) poly(divinylbenzene) (PDVB) cores and (b) core cross-linked star (CCS) clusters, where the differential refractive index (DRI), light scattering (LS) detector, and UV−vis detector (λ = 291 nm) traces are shown. PDVB cores (ai) are identifiable by the presence of a UV signal corresponding to the LS and DRI peak. Reaction with monovinyl monomers results in the formation of CCS clusters (bii) and linear poly(methyl methacrylate) (PMMA) (biii), where the former is identifiable by the presence of the same UV signal characteristic of PDVB cores. Linear PMMA alone does not have a UV signal at the prescribed wavelength. In addition, a very high-M_w species (bi) is observed with a large LS peak; however, its concentration is negligible.

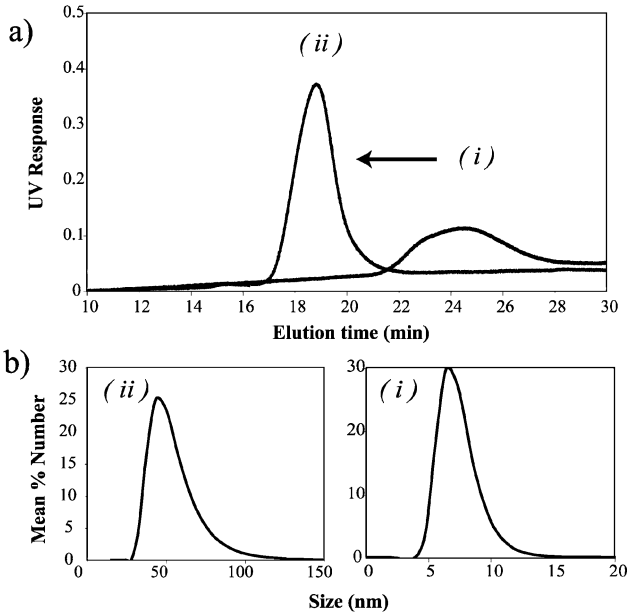

Figure 2. (a) UV signal response from GPC analysis of (i) poly(divinylbenzene) (PDVB) cores and (ii) fractionated core cross-linked star (CCS) clusters. The observed migration of the UV signal is the result of polymerization of PDVB cores with methyl methacrylate (MMA) to form high-M_w CCS clusters, of which the PDVB cores are fully incorporated. (b) Dynamic light scattering analysis of (i) PDVB cores and (ii) fractionated CCS clusters in chloroform shows that the former has a mean diameter of 7.2 nm and the latter a mean diameter of 51.3 nm.

dominated by resonances characteristic of PMMA. The disappearance of resonances characteristic of the PDVB cores is either due to its low content in proportion to the PMMA segments or the reduced segmental mobility of the cores that couples with the linear PMMA segments, similar to the observations by

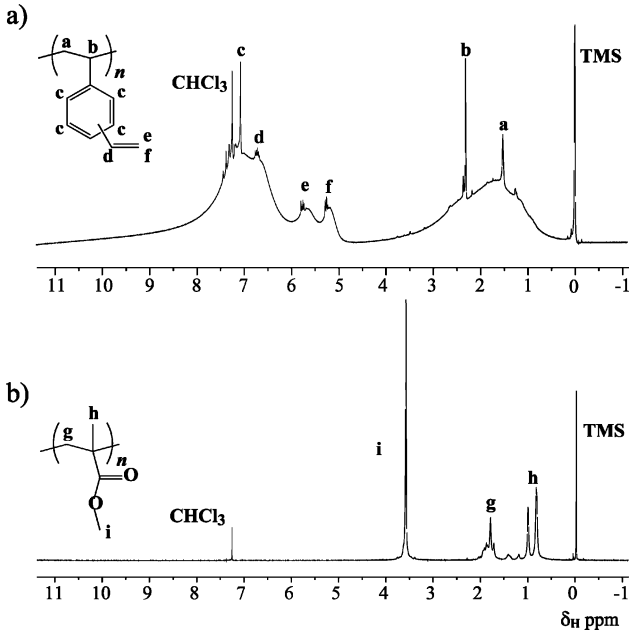

Figure 3. ^{1}H NMR spectra of (a) poly(divinylbenzene) (PDVB) cores and (b) fractionated PMMA−PDVB CCS clusters. After cluster formation, only the characteristic resonances of PMMA are visible.

Sawamoto and co-workers[5] and Wiltshire et al.[13] Similarly, ^{1}H NMR spectroscopic analysis of a (PMMA/10 kDa)$_{108}$−PDVB CCS polymer[18] also resulted in a spectrum dominated by resonances characteristic of PMMA. On the basis of the ^{1}H NMR and GPC-MALLS/UV analysis, it was concluded that the polymeric material formed from reaction of PDVB cores with MMA were PMMA−PDVB copolymers that structurally resemble clusters of CCS polymers.

Kinetics of CCS Cluster Formation. The kinetics of CCS cluster formation was investigated by taking intermediate samples for GPC and GCMS analysis. Parts a and b of Figure 4 are the DRI and UV detector responses, respectively, for samples taken at regular time intervals. Formation of CCS clusters occurs predominantly in the first hour of the reaction, as revealed by the evolution of high-M_w species in the DRI response (Figure 4a) and the migration of the UV absorbance (Figure 4b) corresponding to the aromatic moieties. As a result of the large size of the PDVB cores and high number of unsaturated moieties, they are highly susceptible to attack by propagating radicals in the early stages of polymerization. However, after the first hour, cluster growth increases slowly relative to linear polymer formation as a result of steric hindrance or complete consumption of the vinylic groups of the PDVB cores. The resulting CCS cluster has a M_w of 5254 kDa, a PDI of 1.78, and a relative concentration of 24%. The linear PMMA has a M_w of 49.0 kDa, a PDI of 4.28, and a relative concentration of 76%. The conversion of MMA measured by GCMS was 90%.

The kinetic results were also used to validate the formation of CCS clusters via a simple analysis of M_w and MMA conversion. At t_{rxn} = 0.5 h, MMA conversion was 6.5% as determined by GCMS; i.e., 0.022 mol of MMA has been incorporated into the polymer. Therefore, the average mole ratio of MMA:PDVB cores was 1476:1 (since linear polymer formation was negligible at this time, the observed conversion of MMA was assumed to contribute solely to CCS cluster formation). Therefore, the theoretical M_w was calculated as the sum of 1476 units of MMA and 1 unit of PDVB core ($M_{w,PDVB\ core}$ = 67.07 kDa), i.e., 214.8 kDa. The observed M_w

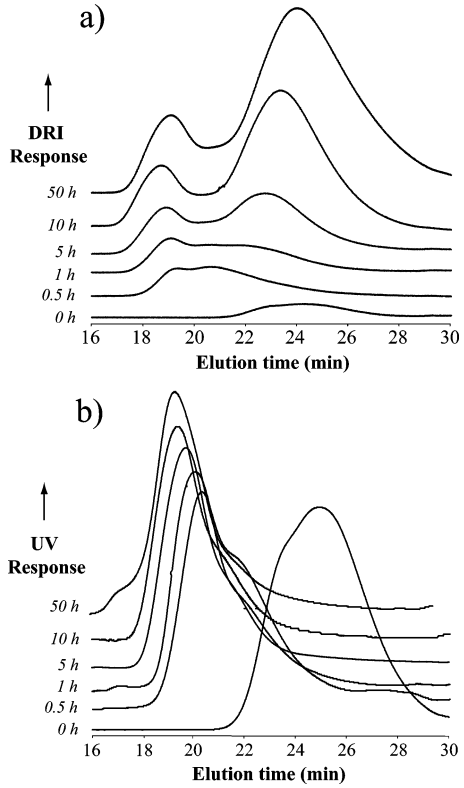

Figure 4. Kinetics of cluster formation followed by GPC analysis: (a) change in differential refractive index (DRI) response with time; (b) change in UV response (λ = 291 nm) with time. Samples were taken at 0, 0.5, 1, 5, 10, and 50 h.

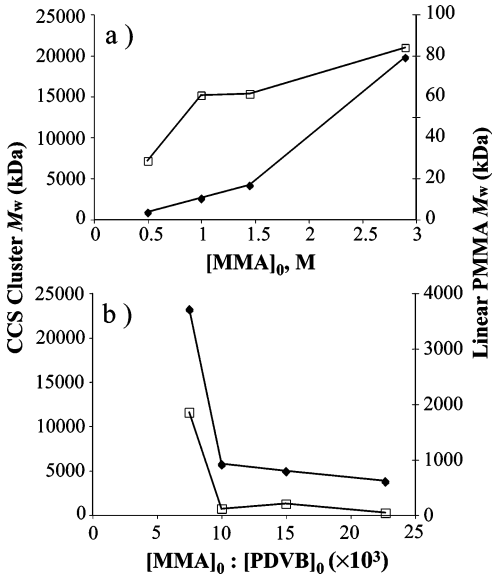

Figure 5. (a) M_w data for core cross-linked star (CCS) clusters (◆) and linear PMMA (□) vs initial concentration of MMA ([MMA]$_0$:[PDVB]$_0$:[AIBN]$_0$ = 22700:1:227). Increasing [MMA]$_0$ results in an increase of CCS cluster and linear PMMA M_w. (b) M_w data for CCS clusters (◆) and linear PMMA (□) vs molar ratio of MMA to PDVB cores ([MMA]$_0$ = 1.45 M, n_{MMA}/n_{AIBN} = 100). An increase in the amount of MMA relative to PDVB cores results in a decrease in CCS cluster and linear PMMA M_w.

was in fact 1609 kDa, which means that formation of covalent bonds between multiple stars must be occurring, with approximately 7.5 cores to each individual cluster (number of clusters = observed M_w/expected M_w, assuming statistical distribution of monomers and PDVB cores).

Effect of Reaction Conditions. The selection of an appropriate formulation is essential to obtain CCS clusters of desired M_w and concentration in the reaction solution. Relevant polymerization data are thus presented in Table 2. Two formulation parameters were investigated to observe the effect on CCS cluster formation: (i) the initial concentration of MMA ([MMA]$_0$) (**3A**−**3D**) and (ii) the mole ratio of MMA to PDVB cores (n_{MMA}/n_{PDVB}) (**3B, 4A**−**4C**).

The initial concentration of MMA was varied between 0.5 and 3.0 M while maintaining the MMA:PDVB mole ratio at 22 700:1 (Figure 5a). As the concentration of MMA was decreased, both the CCS cluster and linear PMMA M_w decreased (**3A**−**3D**); however, the relative cluster concentration remained constant at ∼10%. The MMA:PDVB mole ratio was also varied between 7500:1 and 22 700:1 while maintaining [MMA]$_0$ at 1.45 M (Figure 5b). It was observed that decreasing the MMA:PDVB mole ratio resulted in a increase in the CCS cluster and linear PMMA M_w (**3D, 4A**−**4C**). Furthermore, the relative proportion of CCS clusters also increased. Therefore, it is observed that both [MMA]$_0$ and the MMA:PDVB mole ratio affects the CCS cluster and linear PMMA M_w.

Control of CCS cluster M_w is better achieved by varying [MMA]$_0$ (**3A**−**3D**). By increasing [MMA]$_0$, the CCS cluster and linear PMMA M_w increases from 5000 to 20 000 kDa. The relative concentration of CCS clusters is consistently 10% under these conditions. While the relative concentration of CCS clusters is constant, the total solids content of the polymerization (CCS cluster + linear PMMA) decreases with decreasing [MMA]$_0$. For example, at low [MMA]$_0$ (**3D**), the total percentage solids is 5.2% w/v; hence, the percentage of CCS clusters is 0.4% w/v.

Decreasing the MMA:PDVB mole ratio (**3B, 4A**−**4C**) increases the CCS cluster and linear PMMA M_w. This is because the number of PDVB cores relative to MMA increases as the n_{MMA}/n_{PDVB} is decreased. As a result, the potential for intermolecular cross-linking between propagating CCS clusters is increased and the relative concentration and M_w of CCS clusters also increase. While this is the general trend, there is little variability in CCS cluster and linear PMMA M_w until the ratio n_{MMA}/n_{PDVB} has a value of less than 10 000, where there was a steep increase in M_w.

In summary, the selection of appropriate conditions depends on the desired cluster M_w, concentration in solution, or product yield. Where high M_w and relative cluster proportion is required, a high [MMA]$_0$ and low n_{MMA}/n_{PDVB} may be used. If a high percentage of total solids is required and M_w is not a critical variable, then a high [MMA]$_0$ and high n_{MMA}/n_{PDVB} may be used, where the latter also determines the relative cluster concentration.

Properties of CCS Clusters

Solvent Effect. The macromolecular structure of a CCS cluster is unique in that the multiple loosely cross-linked PDVB cores are held together by linear segments of PMMA. The influence of this segment on CCS cluster dynamics in solution is illustrated by the solvent effect (Figure 6), where the average diameter of CCS cluster **3B** based on scattering intensity (number-average) was measured in a good (chloroform) and poor (*N*,*N*-dimethylformamide (DMF)) solvent for PMMA.

The effect of dissolving polymers in a good solvent is that the degree of solvation and hence the hydrodynamic diameter, D_h, and the intrinsic viscosity increase.[19] For the purposes of comparison, CCS polymers which contain a single core were synthesized and subjected to similar DLS measurements. The

Table 2. Polymerization Data for Core Cross-Linked Star (CCS) Cluster Formation Reactions

			CCS cluster			linear polymer	
polymer[a]	$[MMA]_0$ (M)	n_{MMA}/n_{PDVB} ($\times 10^3$)	M_w[b] (kDa)	PDI[b]	rel conc (%)[b]	M_w[b] (kDa)	PDI[b]
3A	2.90	22.7	19800	1.19	9.9	83.8	1.17
3B	1.45	22.7	4200	1.27	9.6	61.2	1.40
3C	1.00	22.7	2600	1.28	10.9	60.5	1.31
3D	0.50	22.7	885	1.32	9.3	28.5	1.93
4A	1.45	15.0	4975	1.16	18.7	206.5	1.17
4B	1.45	10.0	5756	1.71	18.0	115.6	1.23
4C	1.45	7.5	23210	1.18	23.2	1850.0	1.05

[a] Conventional free-radical polymerization (FRP) of MMA and poly(divinylbenzene) (PDVB) cores was carried out in toluene in the presence of 2,2-azobis(2-methylpropionitrile) (AIBN) at 65 °C. [b] M_w, PDI, and relative concentration were determined by gel permeation chromatography−multiangle laser light scattering (GPC−MALLS). Relative concentration of CCS clusters is expressed as [peak area of clusters/(peak area of clusters and free arms)] × 100%.

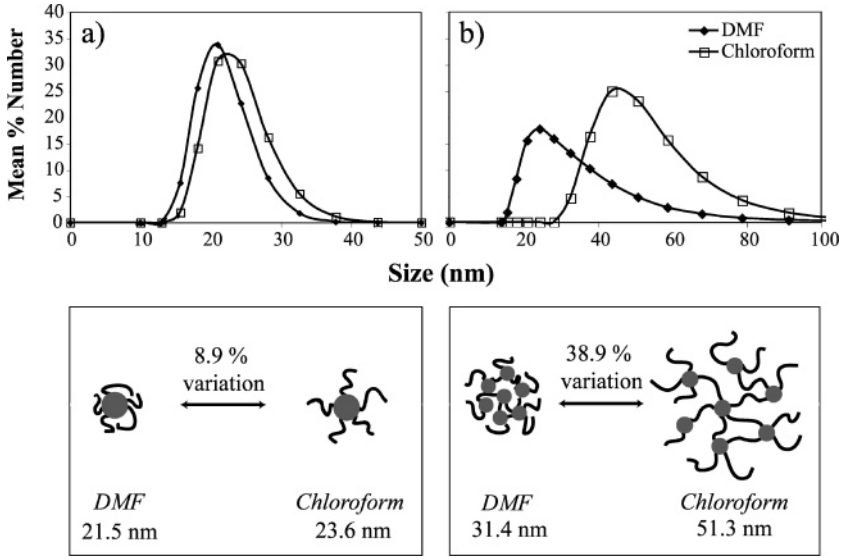

Figure 6. Dynamic light scattering of (a) $(PMMA/21\ kDa)_{21}$−PEGDMA CCS polymer and (b) CCS clusters (**3B**) in chloroform (□) and DMF (◆). $(PMMA/21\ kDa)_{21}$−PEGDMA CCS polymers have a mean diameter of 21.5 nm in DMF and 23.6 nm in chloroform (a 8.9% variation), whereas CCS clusters have a mean diameter of 31.4 nm in DMF and 51.3 nm in chloroform (a 38.9% variation).

$(PMMA/21\ kDa)_{21}$−EGDMA CCS polymer was found to have a mean diameter of 21.5 nm in DMF and 23.6 nm in chloroform, corresponding to an increase in diameter of 8.9% (Figure 6a). Purified CCS clusters have a mean diameter of 31.4 nm in DMF and 51.3 nm in chloroform, corresponding to a 38.9% increase (Figure 6b). Hence, it is apparent that CCS clusters are more responsive to solvent choice compared to CCS polymers. The cores of both the CCS polymer and CCS cluster are unlikely to be a significant contributor to D_h due to their cross-linked nature; thus, their contribution to changes in D_h is minor. Clearly, the solvent effect applies mainly to the linear PMMA segments of the polymers. FRP of MMA and PDVB cores is likely to result in a statistical distribution of PDVB cores within the CCS cluster structure; hence, the change in mean diameters is due to not only the linear segment on the periphery of the CCS cluster but also the linear segments within the interior of the cluster. Therefore, the more dramatic increase in mean diameter for a CCS cluster compared to a CCS polymer may be largely attributed to the high degree of solvation of the linear segment throughout the CCS cluster.

As the unique macromolecular architecture of CCS clusters is strongly influenced by solvent selection, control over its macroscopic properties (such as solution viscosity and refractive index) may be achieved by careful selection of solvent(s). Furthermore, CCS clusters may be designed as stimuli-responsive nanoparticles that have tunable densities due to particle expansion and contraction on the basis of solvent selection. The interior of CCS clusters may also be functionalized and protected by contraction of the cluster, and thus reactivity is impeded or controlled on the basis of solvent manipulation.

Thermal Properties of CCS Clusters. Two methods of thermal analysis were employed to study CCS clusters; modulated differential scanning calorimetry (DSC) was used to determine the polymer glass transition temperature (T_g), and thermogravimetric analysis (TGA) was used to study the thermal degradation behavior. Four polymers with different macromolecular structures were studied: (i) linear PMMA (20.7 kDa) (**T1**), (ii) $(PMMA/10\ kDa)_{108}$−PDVB CCS polymer (1345 kDa, 79% w/w PMMA segment) (**T2**), (iii) PMMA−PDVB CCS clusters (6753 kDa with 67.1 kDa PDVB cores, 92.5% w/w PMMA segment[20]) (**T3**), and (iv) PDVB cores (79.8 kDa) (**T4**).

DSC analysis of the polymers determined that both linear PMMA **T1** (T_g = 127 °C) and CCS polymer **T2** (T_g = 134 °C) displayed T_g's within the expected range for PMMA,[21−24] whereas the CCS cluster **T3** did not display a T_g (Figure 7). The relatively high T_g values (compared to atactic PMMA[22]) displayed by **T1** and **T2** are attributed to the absence of low-M_w oligomers and narrow polydispersities[23] (PDI_{PMMA} = 1.11, $PDI_{CCS\ Polymer}$ = 1.56). Unlike block copolymers that have multiple T_g's according to their particular constituents,[24] CCS polymer **T2** displays a T_g for its PMMA arms only and does not have a core T_g, consistent with the observations of Connal et al.[11] Despite having a similar copolymer composition to **T2**, CCS clusters did not display an apparent T_g. This is possibly due to the high degree of cross-linking of the linear PMMA

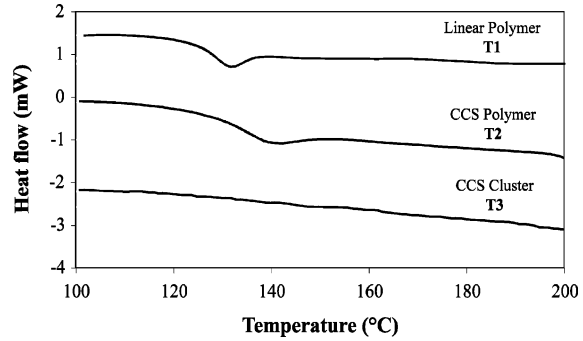

Figure 7. DSC curves for linear PMMA (**T1**), (PMMA/21 kDa)$_{21}$−PDVB CCS polymer (**T2**), and PMMA−PDVB CCS clusters (**T3**).

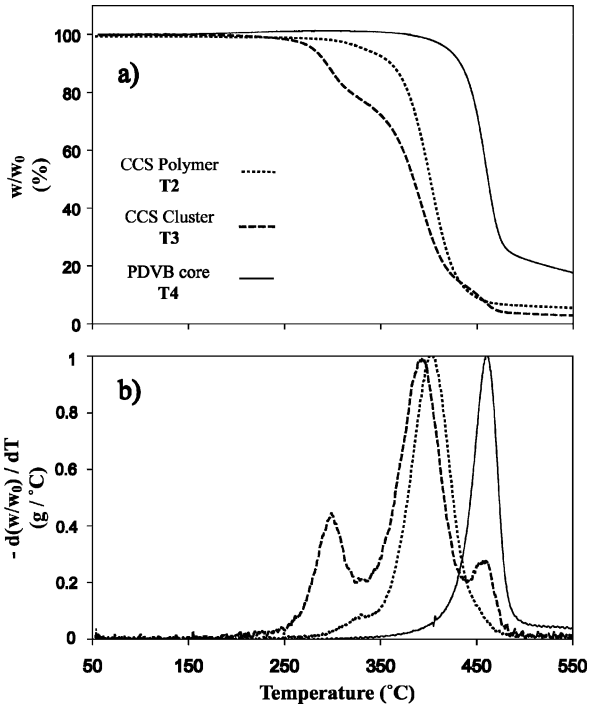

Figure 8. (a) Thermogravimetric (TG) and (b) normalized first-derivative thermogravimetric (DTG) curves for (PMMA/10 kDa)$_{108}$−PDVB CCS polymer (**T2**) (···), PMMA−PDVB CCS clusters (**T3**) (- - -), and PDVB cores (**T4**) (—).

segments to PDVB cores. PDVB cores **T4** were also analyzed as a homopolymer by DSC and found to have no distinct T_g, as a result of its highly cross-linked structure.

The thermal degradation behavior of the polymers **T2**−**T4** were analyzed by TGA and the results illustrated as thermogravimetric (TG) curves (Figure 8a) and derivative thermogravimetric (DTG) curves (Figure 8b). The TG curve is plotted as the percentage weight loss (% w/w_0) with respect to temperature, and the DTG curve is plotted as the first-derivative weight loss ($d(w/w_0)/dT$) with respect to temperature. TG curves provide percentage values of weight loss while DTG curves serve to separate degradation events into distinct peaks. The thermal degradation behavior of linear PMMA synthesized by FRP or living radical polymerization has been widely studied[25−28] and therefore will not be repeated here.

The PDVB cores **T4** were initially analyzed, and it was found that up to 17.6% of residual weight remains after thermal treatment up to 550 °C. In comparison, a PMMA homopolymer is fully degraded after treatment up to the same temperature.[25,26,28] The TG curves for CCS polymer **T2** and CCS cluster **T3** also indicate a residual weight of 5.5% and 2.8%, respectively, indicating that residual weight from the PDVB segments persists, and hence both polymers contain PDVB segments. Thermal degradation of **T3** indicates that there are three main degradation events; this is clearly seen on its DTG curve. The low- (T_{degr} = 300 °C) and intermediate-temperature (T_{degr} = 396 °C) degradation peaks on the DTG curve are caused by radical-induced decomposition of unsaturated PMMA end groups and random scission of the PMMA chain, respectively. This is consistent with observations of Kashiwagi et al.[25] and Manring et al.,[26] who demonstrated that lower T_{degr} are caused by "weak links" in the PMMA chain, i.e., head-to-head linkages and unsaturated end groups that are both products of radical−radical termination. In the case of CCS cluster **T3**, T_{degr} = 300 °C corresponds to unsaturated end groups in the polymer and is expected for polymers synthesized by FRP. In contrast, CCS polymer **T2** has PMMA arms that do not contain defect structures because it was synthesized by ATRP, and hence, its degradation (T_{degr} = 405 °C) was observed to be mainly as a result of random chain scission.[27] Similar observations were made by Moineau et al.,[23] who showed that polymers synthesized by ATRP have better thermal stability. This finding also rules out the PMMA−PDVB linkage as the "weak link" in the macromolecule as both **T2** and **T3** contain the same bonds; however, **T3** is stable up to the T_{degr} for PMMA random chain scission. The degradation of the PDVB core was observed at T_{degr} = 460 °C for both CCS cluster **T3** and PDVB core **T4**; however, a degradation peak for the PDVB core of CCS polymer **T2** was not observed, possibly due to the intensity and overlap of the PMMA degradation peak.

The thermal stability of CCS clusters is high compared to some FRP-synthesized PMMA due to the absence of head-to-head linkages that cause chain instability at relatively low temperatures (<250 °C). Thermal instability of the clusters began at temperatures above 250 °C where radical-induced decomposition of unsaturated PMMA chains at the periphery of the CCS cluster cause partial decomposition, followed by random scission of the remaining PMMA segments at about 400 °C and finally degradation of the PDVB cores at 460 °C. Thermal analysis of (PMMA/10 kDa)$_{108}$−PDVB CCS polymer has shown that a saturated PMMA segment leads to better thermal stability. Potentially, this may be achieved in CCS cluster formation by FRP via addition of a hydrogen-donor chain transfer agent into the reaction formulation; thus, chain termination occurs by hydrogen-atom transfer.[29]

Conclusion

The "core-first" FRP of PDVB cores containing unreacted double bonds with MMA leads to the formation of CCS clusters, in which the PDVB cores are held together in a micronetwork with linear PMMA segments. GPC-MALLS in combination with UV−vis spectrophotometry, DLS, and ^{1}H NMR verifies the formation of the PMMA−PDVB clusters, which attain molecular weights up to several million daltons without phase separation from its solvent, a characteristic of its architecture. In addition, the unique and compact architecture leads to other interesting properties, such as solvent-induced expansion−contraction of the cluster. Thermal analysis by DSC and TGA demonstrate that CCS clusters do not have a well-defined T_g (due to the high degree of cross-linking between the linear PMMA segments and PDVB cores) and that thermal stability is comparable to linear PMMA synthesized using FRP conditions. Further studies are currently being conducted to develop new responsive materials based on this unique type of macromolecule, as the formulation methods described in this study may also be utilized on other organic and inorganic precursors.

Acknowledgment. The authors thank Clem Powell for assistance with DSC experiments and Paul A. Gurr for sample preparation. Funding by the Australian Research Council (ARC) Linkage project supported by DuPont is acknowledged.

Note Added after ASAP Publication. This article was published ASAP on October 9, 2007. The caption to Figure 8 has been modified. The correct version was published on October 15, 2007.

Supporting Information Available: Experimental methods for the synthesis of linear PMMA, $(PMMA/10\ kDa)_{108}$−PDVB, and $(PMMA/21\ kDa)_{21}$−PEGDMA CCS polymer by ATRP; ^1H and ^{13}C NMR spectra for the $(PMMA/10\ kDa)_{108}$−PDVB CCS polymer. This material is available free of charge via the Internet at http://pubs.acs.org.

References and Notes

(1) (a) Hong, Y. E.; Cooper-White, J. J.; Mackay, M. E.; Hawker, C. J.; Malmström, E.; Rehnberg, N. *J. Rheol.* **1999**, *43*, 781−93. (b) Slark, A. T.; Sherrington, D. C.; Titterton, A.; Martin, I. K. *J. Mater. Chem.* **2003**, *13*, 2711−20. (c) O'Brien, N.; McKee, A.; Sherrington, D. C.; Slark, A. T.; Titterton, A. *Polymer* **2000**, *41*, 6027−31. (d) Isaure, F.; Cormack, P. A. G.; Sherrington, D. C. *J. Mater. Chem.* **2003**, *13*, 2701−10. (e) Isaure, F.; Cormack, P. A. G.; Sherrington, D. C. *Macromolecules* **2004**, *37*, 2096−105. (f) Graham, S.; Cormack, P. A. G.; Sherrington, D. C. *Macromolecules* **2005**, *38*, 86−90. (g) Camerlynck, S.; Cormack, P. A. G.; Sherrington, D. C.; Saunders, G. *J. Macromol. Sci., Polym. Phys.* **2005**, *44*, 881−95.

(2) (a) Abrol, S.; Kambouris, P. A.; Looney, M. J.; Solomon, D. H. *Macromol. Rapid Commun.* **1997**, *18*, 755−60. (b) Abrol, S.; Caulfield, M. J.; Qiao, G. G.; Solomon, D. H. *Polymer* **2001**, *42*, 5987−91. (c) Bosman, A. W.; Vestberg, R.; Heumann, A.; Fréchet, J. M. J.; Hawker, C. J. *J. Am. Chem. Soc.* **2003**, *125*, 715−28. (d) Solomon, D. H.; Abrol, S.; Kambouris, P. A.; Looney, M. G. *A Process for Preparing Polymeric Microgels*, WO9831739, 1998.

(3) (a) Gurr, P. A.; Qiao, G. G.; Solomon, D. H. *Macromolecules* **2003**, *36*, 5650−4. (b) Connal, L. A.; Gurr, P. A.; Qiao, G. G.; Solomon, D. H. *J. Mater. Chem.* **2004**, *15*, 1286−92.

(4) (a) Solomon, D. H.; Qiao, G. G.; Abrol, S. *Process for Microgel Preparation*, WO9958588, 1999. (b) Zhang, X.; Xia, J. H.; Matyjaszewski, K. *Macromolecules* **2000**, *33*, 2340−5. (c) Xia, J. H.; Zhang, X.; Matyjaszewski, K. *Macromolecules* **1999**, *32*, 4482−4. (d) Baek, K. Y.; Kamigaito, M.; Sawamoto, M. *Macromolecules* **2001**, *34*, 215−21. (e) Baek, K. Y.; Kamigaito, M.; Sawamoto, M. *Macromolecules* **2001**, *34*, 7629−35. (f) Baek, K. Y.; Kamigaito, M.; Sawamoto, M. *J. Polym. Sci., Polym. Chem.* **2002**, *40*, 1972−82. (g) Baek, K. Y.; Kamigaito, M.; Sawamoto, M. *J. Polym. Sci., Polym. Chem.* **2002**, *40*, 633−41. (h) Gao, H.; Ohno, S.; Matyjaszewski, K. *J. Am. Chem. Soc.* **2006**, *128*, 15111−3.

(5) Baek, K. Y.; Kamigaito, M.; Sawamoto, M. *Macromolecules* **2002**, *35*, 1493−8.

(6) (a) Lord, H. T.; Quinn, J. F.; Angus, S. D.; Whittaker, M. R.; Stenzel, M. H.; Davis, T. P. *J. Mater. Chem.* **2003**, *13*, 2819−24. (b) Moad, G.; Mayadunne, R. T. A.; Rizzardo, E.; Skidmore, M.; Thang, S. *Macromol. Symp.* **2003**, *192*, 1−12. (c) Zheng, G. H.; Pan, C. Y. *Polymer* **2005**, *46*, 2802−10.

(7) (a) Kennedy, J. P.; Jacob, S. *Acc. Chem. Res.* **1998**, *31*, 835−41. (b) Sutherland, R. J.; Rhodes, R. B. *Dispersant viscosity index improvers*, US5360564, 1994.

(8) "Core cross-linked star (CCS) polymers" refer to the unique macromolecular structure that consists of a cross-linked core with radiating arms. This macromolecule may also be referred to as star microgels or star nanogels; however, the precise term serves as a disambiguation from other macromolecular architectures, e.g., star polymers.

(9) Peppas, N.; Nagai, T.; Miyajima, M. *Pharm. Tech. Jpn.* **1994**, *10*, 611−7.

(10) Ho, A. K.; Iin, I.; Gurr, P. A.; Mills, M. F.; Qiao, G. G. *Polymer* **2005**, *46*, 6727−35.

(11) Connal, L. A.; Qiao, G. G. *Adv. Mater.* **2006**, *18*, 3024−8.

(12) Wiltshire, J. T.; Qiao, G. G. *Macromolecules* **2006**, *39*, 4282−5.

(13) Wiltshire, J. T.; Qiao, G. G. *Macromolecules* **2006**, *39*, 9018−27.

(14) (a) Shashoua, V. A.; Beaman, R. G. *J. Polym. Sci.* **1958**, *33*, 101−17. (b) Ma, G. H.; Fukutomi, T. *J. Appl. Polym. Sci.* **1991**, *43*, 1451−7. (c) Rodriguez, B. E.; Wolfe, M. S.; Fryd, M. *Macromolecules* **1994**, *27*, 6642−7.

(15) (a) Okay, O.; Naghash, H. J. *Polym. Bull. (Berlin)* **1994**, *33*, 665−72. (b) Dusek, K.; Matejka, L.; Spacek, L.; Winter, H. *Polymer* **1996**, *37*, 2233−42.

(16) Okay, O.; Kurz, M.; Lutz, K.; Funke, W. *Macromolecules* **1995**, *28*, 2728−37.

(17) PDVB cores have a λ_{max} at 253 and 291 nm; however, the latter was selected to prevent overlap with the UV absorption of PMMA.

(18) ^1H and ^{13}C NMR spectra of the $(PMMA/10)_{108}$−PDVB CCS polymer are provided in the Supporting Information.

(19) (a) Cowie, J. M. G. *J. Polym. Sci., Part C* **1968**, *23*, 267−76. (b) Paul, D. R.; St. Lawrence, J. E.; Troell, J. H. *Polym. Eng. Sci.* **1970**, *10*, 70−8.

(20) The CCS clusters used in the DSC study were obtained from the kinetic study. Based on the calculations shown in that section, the number of cores was 7.5; thus, the weight fraction of arms may be calculated as follows: $WF_{PMMA} = 1 - (M_{w,CCS\ cluster}/(\text{number of PDVB cores} \times M_{w,PDVB})$.

(21) (a) Fernandez-Garcia, M.; Lopez-Gonzalez, M. M. C.; Barrales-Rienda, J. M.; Madruga, E. L.; Arias, C. *J. Polym. Sci., Polym. Phys.* **1995**, *32*, 1191−203. (b) Pomposo, J. A.; Eguiazabal, I.; Calahorra, E.; Cortazar, M. *Polymer* **1993**, *34*, 95−102.

(22) (a) Kulik, A. S.; Beckham, H. W.; Schmidt-Rohr, K.; Radloff, D.; Pawelzik, U.; Boeffel, C.; Spiess, H. W. *Macromolecules* **1994**, *27*, 4746−54. (b) Wu, S. *J. Appl. Polym. Sci.* **1992**, *46*, 619−24.

(23) Moineau, G.; Minet, M.; Dubois, Ph.; Teyssié, Ph.; Senninger, T.; Jérôme, R. *Macromolecules* **1999**, *32*, 27−35.

(24) (a) Yu, J. M.; Dubois, Ph.; Teyssié, Ph.; Jérôme, R. *Macromolecules* **1996**, *29*, 6090−9. (b) Brown, D. A.; Price, G. J. *Polymer* **2001**, *42*, 4767−71.

(25) (a) Kashiwagi, T.; Hirata, T.; Brown, J. E. *Macromolecules* **1985**, *18*, 131−8. (b) Hirata, T.; Kashiwagi, T.; Brown, J. E. *Macromolecules* **1985**, *18*, 1410−8. (c) Kashiwagi, T.; Inaba, A.; Brown, J. E.; Hatada, K.; Kitayama, T.; Masuda, E. *Macromolecules* **1986**, *19*, 2160−8.

(26) (a) Manring, L. E. *Macromolecules* **1988**, *21*, 528−30. (b) Manring, L. E. *Macromolecules* **1989**, *22*, 2673−7. (c) Manring, L. E.; Sogah, D. Y.; Cohen, G. M. *Macromolecules* **1989**, *22*, 4652−4. (d) Manring, L. E. *Macromolecules* **1991**, *24*, 3304−9.

(27) Hatada, K.; Kitayama, T.; Fujimoto, N.; Nishiura, T. *J. Macromol. Sci., Pure Appl. Chem.* **1993**, *30*, 645−67.

(28) (a) Granel, C.; Dubois, Ph.; Jérôme, R.; Teyssié, Ph. *Macromolecules* **1996**, *29*, 8576−82. (b) Wunderlich, W.; Benfaremo, N.; Klapper, M.; Müllen, K. *Macromol. Rapid Commun.* **1996**, *17*, 433−8. (c) Colombani, D.; Steenbock, M.; Klapper, M.; Müllen, K. *Macromol. Rapid Commun.* **1997**, *18*, 243−51.

(29) Bagby, G.; Lehrle, R. S.; Robb, J. C. *Polymer* **1969**, *10*, 683−90.

MA070996Z